Entropy Functional Based Online Adaptive Decision Fusion Framework with Application to Wildfire Detection in Video

Osman Günay*, Behçet Uğur Töreyin†, Kıvanç Köse* and A. Enis Çetin*
*Department of Electrical and Electronics Engineering
Bilkent University, Ankara, Turkey, 06800
Telephone: +90-312-290-1219 Fax: +90-312-266-4192
Email: {osman,kkivanc}@ee.bilkent.edu.tr, cetin@bilkent.edu.tr
†Department of Electronic and Communication Engineering
Çankaya University
Telephone:+90-312-233-1330
Email: toreyin@cankaya.edu.tr

(EDICS:) ARS-IIU:Image & Video Interpretation and Understanding Object recognition and classification; Foreground/background segregation; Scene analysis

***Abstract*—In this paper, an entropy functional based online adaptive decision fusion framework is developed for image analysis and computer vision applications. In this framework, it is assumed that the compound algorithm consists of several sub-algorithms, each of which yields its own decision as a real number centered around zero, representing the confidence level of that particular sub-algorithm. Decision values are linearly combined with weights which are updated online according to an active fusion method based on performing entropic projections onto convex sets describing sub-algorithms. It is assumed that there is an oracle, who is usually a human operator, providing feedback to the decision fusion method. A video based wildfire detection system was developed to evaluate the performance of the decision fusion algorithm. In this case, image data arrives sequentially and the oracle is the security guard of the forest lookout tower, verifying the decision of the combined algorithm. The simulation results are presented.**

***Index Terms*—Projections onto convex sets, active learning, decision fusion, online learning, entropy maximization, wildfire detection using video.**

I. Introduction

In this paper an online learning framework, called Entropy Functional based Adaptive Decision Fusion (EADF), which can be used in various image analysis and computer vision applications is proposed. In this framework, it is assumed that the compound algorithm consists of several sub-algorithms each of which yields its own decision. The final decision is reached based on a set of real numbers representing confidence levels of various sub-algorithms. Decision values are linearly combined with weights that are updated online using an active fusion method based on performing entropic projections (e-projections) onto convex sets describing the sub-algorithms.

Adaptive learning methods based on orthogonal projections are successfully used in some computer vision and pattern recognition problems [1], [2]. A multiple classifier system is useful for difficult pattern recognition problems, especially when large class sets and noisy data are involved, by allowing the use of arbitrary feature descriptors and classification procedures at the same time [3]. Instead of determining the weights using orthogonal projections as in [1], [2], we introduce the entropic e-projection approach which is based on a generalized projection onto a convex set.

The studies in the field of collective recognition, which were started in the mid 1950s, found wide application in practice during the last decade, leading to solutions to complex, large-scale applied problems [4]. One of the first examples of the use of multiple classifiers was given by Dasarathy in [5] in which he introduced the concept of composite classifier systems as a means of achieving improved recognition system performance compared to employing the classifier components individually. The method is illustrated by studying the case of the linear/NN(Nearest Neighbor) classifier composite system. Kumar and Zhang used multiple classifiers for palmprint recognition by characterizing the user's identity through the simultaneous use of three major palmprint representations and achieved better performance than either one individually [6]. A multiple classifier fusion algorithm is proposed for developing an effective video based face recognition method [7]. Garcia and Puig present results showing that pixel-based texture classification can be significantly improved by integrating texture methods from multiple families, each evaluated over multisized windows [8]. This technique consists of an initial training stage that evaluates the behavior of each considered texture method when applied to the given texture patterns of interest over various evaluation windows of different size.

In this article, the EADF framework is applied to a computer vision based wildfire detection problem. The system based on this method is currently being used in more than 60 forest fire lookout towers in the Mediterranean region. The proposed automatic video based wildfire detection algorithm is based on five sub-algorithms: (i) slow moving video object detection, (ii) smoke-colored region detection, (iii) wavelet transform based region smoothness detection, (iv) shadow detection and elimination, (v) covariance matrix based classification. Each sub-algorithm decides on the existence of smoke in the viewing range of the camera separately. Decisions from sub-algorithms are combined with the adaptive decision fusion method. Initial weights of the sub-algorithms are determined from actual forest fire videos and test fires. They are updated by using entropic e-projections onto hyperplanes defined by the fusion weights. It is assumed that there is an oracle monitoring the decisions of the combined algorithm. In the wildfire detection case, the oracle is a security guard. Whenever a fire is detected the decision should be acknowledged by the security guard. The decision algorithm will also produce false alarms in practice. Whenever an alarm occurs, the system asks the security guard to verify its decision. If it is incorrect the weights are updated according to the decision of the security guard. The goal of the system is not to replace the security guard, but to provide a supporting tool to help him or her. The attention span of a typical security guard is only 20 minutes in monitoring stations. It is also possible to use feedback at specified intervals and run the algorithm autonomously at other times. For example, the weights can be updated when there is no fire in the viewing range of the camera and then the system can be run without feedback.

The paper is organized as follows: Entropy functional based Adaptive Decision Fusion (EADF) framework is described in Section II. The first part of this section describes our previous weight update algorithm which is obtained by orthogonal projections onto hyperplanes [1], the second part proposes an entropy based e-projection method for weight update of the sub-algorithms. Section III introduces the video based wildfire detection problem. In Section IV, each one of the five sub-algorithms which make up the compound (main) wildfire detection algorithm are described. In Section V, experimental results are presented and the proposed online active fusion method is compared with the universal linear predictor and the weighted majority algorithms. The proposed framework is not restricted to the wildfire detection problem. It can also be used in other real-time intelligent video analysis applications in which a security guard is available. The proposed EADF method is also evaluated on a dataset from the UCI machine learning repository [9]. Well-known classifiers (SVM, K-NN) are combined using EADF. During the training stage, individual decisions of classifiers are used to find the weight of each classifier in the composite EADF classifier. Finally, conclusions are drawn in Section VI.

II. Adaptive Decision Fusion (ADF) Framework

Let the compound algorithm be composed of M-many detection sub-algorithms: $D_1, ..., D_M$. Upon receiving a sample input x at time step n, each sub-algorithm yields a decision value $D_i(x,n) \in \mathbb{R}$ centered around zero. If $D_i(x,n) > 0$, it means that the event is detected by the i-th sub-algorithm. Otherwise, it is assumed that the event did not happen. The type of the sample input x may vary depending on the algorithm. It may be an individual pixel, or an image region, or the entire image depending on the sub-algorithm of the computer vision problem. For example, in the wildfire detection problem presented in Section III, the number of sub-algorithms is M=5 and each pixel at the location x of incoming image frame is considered as a sample input for every detection algorithm.

Let $\mathbf{D}(x,n) = [D_1(x,n), ..., D_M(x,n)]^T$, be the vector of decision values of the sub-algorithms for the pixel at location x of input image frame at time step n, and $\mathbf{w}(x,n) = [w_1(x,n), ..., w_M(x,n)]^T$ be the current weight vector. For simplicity we will drop x in $\mathbf{w}(x,n)$ for the rest of the paper.

We define

$$\hat{y}(x,n) = \mathbf{D^T}(x,n)\mathbf{w}(n) = \sum_i w_i(n) D_i(x,n) \tag{1}$$

as an estimate of the correct classification result $y(x,n)$ of the oracle for the pixel at location x of input image frame at time step n, and the error $e(x,n)$ as $e(x,n) = y(x,n) - \hat{y}(x,n)$. As it can be seen in the next subsection, the main advantage of the proposed algorithm compared to other related methods in [10], [11], [12], is the controlled feedback mechanism based on the error term. Weights of the algorithms producing an incorrect (correct) decision is reduced (increased) iteratively at each time step. Another advantage of the proposed algorithm is that it does not assume any specific probability distribution about the data.

A. Set Theoretic Weight Update Algorithm based on Orthogonal Projections

In this subsection, we first review the orthogonal projection based weight update scheme [1]. Ideally, weighted decision values of sub-algorithms should be equal to the decision value of $y(x,n)$ the oracle:

$$y(x,n) = \mathbf{D}^T(x,n)\mathbf{w} \tag{2}$$

which represents a hyperplane in the M-dimensional space, $\mathbb{R}^M$. Hyperplanes are closed and convex in $\mathbb{R}^M$. At time instant n, $\mathbf{D}^T(x,n)\mathbf{w}(n)$ may not be equal to $y(x,n)$. In our approach, the next set of weights are determined by projecting the current weight vector $\mathbf{w}(n)$ onto the hyperplane represented by Eq. 2. The orthogonal projection $\mathbf{w}(n+1)$ of the vector of weights $\mathbf{w}(n) \in \mathbb{R}^M$ onto the hyperplane $y(x,n) = \mathbf{D}^T(x,n)\mathbf{w}$ is the closest vector on the hyperplane to the vector $\mathbf{w}(n)$.

Let us formulate the problem as a minimization problem:

$$\begin{gathered}\min_{\mathbf{w}^*} \|\mathbf{w}^* - \mathbf{w}(n)\|_2 \\ \text{subject to } \mathbf{D}^T(x,n)\mathbf{w}^* = y(x,n)\end{gathered} \tag{3}$$

The solution can be obtained by using Lagrange multipliers. The solution is called the metric projection mapping solution. However we use the term orthogonal projection because the line going through $\mathbf{w}^*$ and $\mathbf{w}(n)$ is orthogonal to the hyperplane. If we define the next set of weights as $\mathbf{w(n+1)} = \mathbf{w}^*$ it can be obtained by the following iteration:

$$\mathbf{w}(n+1) = \mathbf{w}(n) + \frac{e(x,n)}{\|\mathbf{D}(x,n)\|_2^2}\mathbf{D}(x,n) \tag{4}$$

Hence, the projection vector is calculated according to Eq. 4. Note that Eq. 4 is identical to the normalized least mean square (NLMS) algorithm with update parameter $\mu = 1$. In the NLMS algorithm $0 < \mu < 2$ should be satisfied for convergence [13]. According to the projection onto convex sets (POCS) theory, when there are a finite number of convex sets, repeated cyclical projections onto these sets converge to a vector in the intersection set [14], [15], [16], [17], [18]. The case of an infinite number of convex sets is studied in [2], [19], [20]. They propose to use the convex combination of the projections onto the most recent q sets for online adaptive algorithms [2]. In Section II-C the block projection version of the algorithm that deals with the case when there are an infinite number of convex sets is presented.

Whenever a new input arrives, another hyperplane based on the new decision values $\mathbf{D}(x, n)$ of sub-algorithms, is defined in $\mathbb{R}^M$

$$y(x, n+1) = \mathbf{D}^T(x, n+1)\mathbf{w}^* \tag{5}$$

This hyperplane will not be the same as $y(x, n) = \mathbf{D}^T(x, n)\mathbf{w}(n)$ hyperplane in general. The next set of weights, $\mathbf{w}(n+2)$, are determined by projecting $\mathbf{w}(n+1)$ onto the hyperplane in Eq. 5. When there are a finite number of hyperplanes, iterated weights that are obtained by cyclic projections onto these hyperplanes converge to the intersection of hyperplanes [14], [21], [22].

The pseudo-code of the orthogonal projections onto hyperplanes based algorithm is given in Algorithm 1 which summarizes the projection onto one hyperplane. The block diagram of the algorithm for wildfire detection problem is shown in Fig. 4. The weights are initialized before the first sample arrives. Then for each incoming sample the orthogonal projection algorithm is performed to find the new set of weights. The weights are adjusted so that their sum is 1. The estimated output $\hat{y}(x, n)$ is passed through a nonlinear function to find the classification result for the current sample.

The relation between support vector machines and orthogonal projections onto halfplanes was established in [17], [23] and [24]. As pointed out in [23] SVM is very successful in batch settings, but it cannot handle online problems with drifting concepts in which the data arrive sequentially.

Algorithm 1 The pseudo-code for the POCS based algorithm

```
for $i$ = 1 to M do
  $w_i(0) = \frac{1}{M}$, Initialization
end for
For each sample at time step n.
$e(x, n) = y(x, n) - \hat{y}(x, n)$
for $i$ = 1 to M do
  $w_i(n) \leftarrow w_i(n) + \mu \frac{e(x,n)}{\|\mathbf{D}(x,n)\|_2^2} D_i(x, n)$
end for
for $i$ = 1 to M do
  $w_i(n) \leftarrow \frac{w_i(n)}{\sum_j w_j(n)}$
end for
$\hat{y}(x, n) = \sum_i w_i(n) D_i(x, n)$
if $\hat{y}(x, n) \geq 0$ then
  return 1
else
  return -1
end if
```

B. Entropic Projection (E-Projection) Based Weight Update Algorithm

The l_1 norm based minimization approaches provide successful signal reconstruction results in compressive sensing problems [25], [26], [27], [28]. However, the l_0 and l_1 norm based cost functions used in compressive sensing problems are not differentiable everywhere. The entropy functional approximates the l_1 norm $\sum_i |w_i(n)|$ for $w_i(n) > 0$ [29]. Therefore, it can be used to find approximate solutions to the inverse problems defined in [25], [26] and other applications requiring l_1 norm minimization. Bregman developed convex optimization algorithms in the 1960's and his algorithms are widely used in many signal reconstruction and inverse problems [15], [30], [31], [32], [33], [22], [2]. Bregman's method provides globally convergent iterative algorithms for problems with convex, continuous and differentiable cost functionals $g(.)$:

$$\min_{\mathbf{w} \in C} \; g(\mathbf{w}) \tag{6}$$

such that

$$\mathbf{D}^T(x, n)\mathbf{w}(n) = y \text{ for each time index } n \tag{7}$$

In the EADF framework, the cost function is $g(\mathbf{w}) = \sum_i^M w_i(n) log(w_i(n))$ and each equation in (7) represents a hyperplane $H(x, n) \in \mathbb{R}^M$ which is a closed and convex set. In Bregman's method, the iterative algorithm starts with an arbitrary initial estimate and successive e-projections are performed onto the hyperplanes $H(x, n)$, $n = 1, 2, ..., N$ in each step of the iterative algorithm in a cyclic manner. In this case, we may have infinitely many hyperplanes but we will still use Bregman's e-projection approach.

The e-projection onto a closed and convex set is a generalized version of the metric projection mapping onto a convex set [29]. Let $\mathbf{w}(n)$ denote the weight vector for the n_{th} sample. Its' e-projection $\mathbf{w}^*$ onto a closed convex set C with respect to a cost functional $g(\mathbf{w})$ is defined as follows:

$$\mathbf{w}^* = \arg\min_{\mathbf{w} \in C} \; L(\mathbf{w}, \mathbf{w}(n)) \tag{8}$$

where

$$L(\mathbf{w},\mathbf{w}(n)) = g(\mathbf{w}) - g(\mathbf{w}(n)) - \langle \bigtriangledown g(\mathbf{w}), \mathbf{w} - \mathbf{w}(n)\rangle \quad (9)$$

and $\langle .,. \rangle$ represents the inner product.

In the adaptive learning problem, we have a hyperplane $H(x,n) : \mathbf{D}^T(x,n).\mathbf{w}(n+1) = y(x,n)$ for each sample x. For each hyperplane $H(x,n)$, the e-projection (8) is equivalent to

$$\bigtriangledown g(\mathbf{w}(n+1)) = \bigtriangledown g(\mathbf{w}(n)) + \lambda \mathbf{D}(\mathbf{x},\mathbf{n}) \quad (10)$$

$$\mathbf{D}^T(x,n).\mathbf{w}(n+1) = y(x,n) \quad (11)$$

where λ is the Lagrange multiplier. As pointed out above, the e-projection is a generalization of the metric projection mapping. When the cost functional is the Euclidean cost functional $g(\mathbf{w}) = \sum_i w_i(n)^2$ the distance $L(\mathbf{w_1},\mathbf{w_2})$ becomes the l_2 norm square of the difference vector $(\mathbf{w_1} - \mathbf{w_2})$, and the e-projection simply becomes the well-known orthogonal projection onto a hyperplane.

When the cost functional is the entropy functional $g(\mathbf{w}) = \sum_i w_i(n)\log(w_i(n))$, the e-projection onto the hyperplane $H(x,n)$ leads to the following update equations:

$$w_i(n+1) = w_i(n)e^{\lambda D_i(x,n)},\ i = 1,2,...,M \quad (12)$$

where the Lagrange multiplier λ is obtained by inserting (12) into the hyperplane equation:

$$\mathbf{D}^T(x,n)\mathbf{w}(n+1) = y(x,n) \quad (13)$$

because the e-projection $\mathbf{w}(n+1)$ must be on the hyperplane $H(x,n)$ in Eq. 11. When there are three hyperplanes, one cycle of the projection algorithm is depicted in Fig. 1. If the projections are continued in a cyclic manner the weights will converge to the intersection of the hyperplanes, w_c.

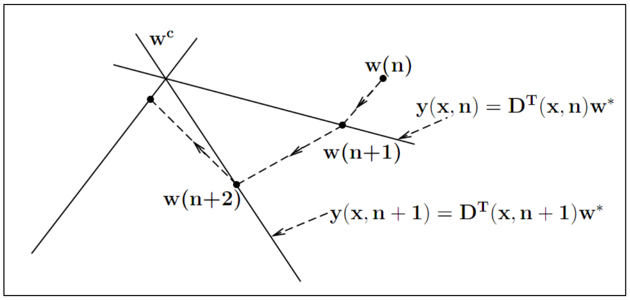

Fig. 1. Geometric interpretation of the entropic-projection method: Weight vectors corresponding to decision functions at each frame are updated to satisfy the hyperplane equations defined by the oracle's decision $y(x,n)$ and the decision vector $\mathbf{D}(x,n)$. Lines in the figure represent hyperplanes in $\mathbb{R}^M$. Weight update vectors converge to the intersection of the hyperplanes. Notice that e-projections are not orthogonal projections.

The above set of equations are used in signal reconstruction from Fourier Transform samples and the tomographic reconstruction problem [16], [30]. The entropy functional is defined only for positive real numbers which coincides with our positive weight assumption.

To find the value of λ at each iteration a nonlinear equation has to be solved (Eqs. 12 and 13). In [34], globally convergent algorithms are developed without finding the exact value of the Lagrange multiplier λ. However, the tracking performance of the algorithm is very important. Weights have to be rapidly updated according to the oracle's decision.

In our application, we first use the second order Taylor series approximation of $e^{\hat{\lambda} D_i(x,n)}$ from Eq. 12 and obtain:

$$w_i(n+1) \approx w_i(n)(1+\hat{\lambda}D_i(x,n)+\frac{\hat{\lambda}^2 D_i^2(x,n)}{2}),\ i = 1,2,...,M \quad (14)$$

Multiplying both sides by $D_i(x,n)$, summing over i and using Eq. 13 we get the following equation:

$$y(x,n) \approx \left(1 + \hat{\lambda}\sum_{i=1}^{M} D_i(x,n)w_i(n) + \hat{\lambda}^2 \sum_{i=1}^{M} \frac{D_i^2(x,n)w_i(n)}{2}\right) \quad (15)$$

We can solve for the initial value of λ from Eq. 15 analytically. We insert the two solutions of Eq. 15 into Eq. 12 and pick the $\mathbf{w}(n+1)$ vector closest to the hyperplane in Eq. 13. This is determined by checking the error $e(x,n)$. We experimentally observed that this estimate provides convergence in forest fire application. To determine a more accurate value of Lagrange multiplier λ we developed a heuristic search method based on the estimate $\hat{\lambda}$. If $e(x,n) < 0$, we choose $\lambda_{min} = \hat{\lambda} - 2|\hat{\lambda}|$, $\lambda_{max} = \hat{\lambda}$ and if $e(x,n) > 0$, we choose $\lambda_{min} = \hat{\lambda}$, $\lambda_{max} = \hat{\lambda} + 2|\hat{\lambda}|$ as the upper and lower bounds of the search window. We only look at R values uniformly distributed between these limits to find the best $\hat{\lambda}$ that produces the lowest error. In our wildfire detection application, we use $R = 4$ as the length of the search window. We could have used a fourth order Taylor series approximation in Eq. 14 and still obtained an analytical solution. After fourth order approximations, a solution has to be numerically found. There are very efficient polynomial root finding algorithms in the literature.

The pseudo-code for the e-projection based adaptive decision fusion based algorithm is given in Algorithm 2, which explains projection onto one hyperplane. In the Algorithm λ_{min} and λ_{max} are determined from the Taylor series approximation as described above. The temporary variables $\mathbf{v}$ and $\mathbf{w_T}$ are used to find the λ value that produces the lowest error. A different λ value is determined for each sample at each time step. Obviously a new value of λ has to be computed whenever a new observation x arrives.

Instead of the Shannon entropy $xlogx$, it is possible to use the regular entropy function $logx$ as the cost functional [34]. In this case,

$$g(\mathbf{w}) = -\sum_i \log(w_i(n)) \quad (16)$$

which is convex for $w_i(n) > 0$. The e-projection onto the hyperplane $H(x,n)$ can be obtained as follows:

$$w_i(n+1) = \frac{w_i(n)}{1+\lambda w_i(n)D_i(x,n)},\ i = 1,2,...,M \quad (17)$$

where the update parameter λ can again be obtained by inserting Eq. 17 into the hyperplane constraint in Eq. 13.

Penalizing the $w_i(n) = 0$ case with an infinite cost may not be suitable for online adaptive fusion problems. However, the cost function:

$$g(\mathbf{w}) = -\sum_i \log(w_i(n)+1) \quad (18)$$

Algorithm 2 The pseudo-code for the EADF algorithm

```
for $i$ = 1 to M do
  $w_i(0) = \frac{1}{M}$, Initialization
end for
For each sample at time step n.
for $\lambda$ = $\lambda_{min}$ to $\lambda_{max}$ do
  for $i$ = 1 to M do
    $v_i(n) = w_i(n)$
    $v_i(n) \leftarrow v_i(n)e^{\lambda D_i(x,n)}$
  end for
  if $\|y(x,n) - \sum_i v_i(n)D_i(x,n)\|_2 < \|y(x,n) - \sum_i w_i(n)D_i(x,n)\|_2$ then
    $\mathbf{w_T}(n) \leftarrow \mathbf{v}(n)$
  end if
end for
$\mathbf{w}(n) \leftarrow \mathbf{w_T}(n)$
for $i$ = 1 to M do
  $w_i(n) \leftarrow \frac{w_i(n)}{\sum_j w_j(n)}$
end for
$\hat{y}(x,n) = \sum_i w_i(n)D_i(x,n)$
if $\hat{y}(x,n) \geq 0$ then
  return 1
else
  return -1
end if
```

is always positive, convex and differentiable for $w_i(n) \geq 0$

In this case, weight update equation becomes:

$$w_i(n+1) = \frac{w_i(n) - \lambda(w_i(n)+1)D_i(x,n)}{1 + \lambda(w_i(n)+1)D_i(x,n)},\ i = 1, 2, ..., M \tag{19}$$

where the update parameter λ should be determined using by substituting Eq. 19 into Eq. 13. Finding the exact value of λ when Eq. 13 is only a four dimensional hyperplane, using numerical methods is not difficult. In the forest fire detection problem we have only five sub-algorithms. However, when the number of sub-algorithms are high, new numerical methods should be determined for cost functions in Eqs. 16 and 18.

For the wildfire detection problem it is desirable that each sub-algorithm should contribute to the compound algorithm because they characterize a feature of wildfire smoke. Therefore weights of algorithms should be between 0 and 1. We want to penalize extreme weight values 0 and 1 more compared to values in between. The entropy functional achieves this. On the other hand the commonly used Euclidean norm penalizes high weight values more compared to zero weight.

C. Block Projection Method

Block projection based methods are developed for inverse problems and active fusion methods [2], [19], [20], [30]. In this case, sets are assumed to arrive sequentially and q of the most recently received observation sets are used to update the weights in the block projection approach. Adaptive projected subgradient method (APSM) works by taking a convex combination of the projections of the current weight vector onto those q sets. The weights calculated using this method are shown to converge to the intersection of hyperplanes [2], i.e, for each sample x there exist $\mathbf{w}^*$ such that:

$$\mathbf{w}^* \in \bigcap_{n \geq n_0} H(x,n) \tag{20}$$

where $n_0 \in \mathbb{N}$.

The next values of weights $\mathbf{w}(n+1)$ can be calculated from the q projections $P_{H(x,j)}(\mathbf{w}(n))$ for $j \in S_n = \{n-q+1, n-q+2, \ldots, n\}$ using the APSM as follows:

$$\mathbf{w}(n+1) = \mathbf{w}(n) + \mu_n \left(\sum_{j \in S_n} \alpha_j(n) P_{H(x,j)}(\mathbf{w}(n)) - \mathbf{w}(n) \right) \tag{21}$$

where $\alpha_j(n)$ is a weight used to control the contribution of the projection onto j_{th} hyperplane and $\sum_{j \in S_n} \alpha_j(n) = 1$, any μ_n can be chosen from $(0, 2\mathcal{M}_n)$ where:

$$\mathcal{M}_n = \frac{\sum_{j \in S_n} \alpha_j(n) \|P_{H(x,j)}(\mathbf{w}(n)) - \mathbf{w}(n)\|_2}{\| \sum_{j \in S_n} \alpha_j(n) P_{H(x,j)}(\mathbf{w}(n)) - \mathbf{w}(n)\|_2} \tag{22}$$

The weights of projections are usually chosen as $\alpha_j(n) = 1/q$ and μ_n can be chosen as 1 since $\mathcal{M}_n \geq 1$ is always true [2]. Both orthogonal and entropic projections can be used as the projection operator, $P_{H(x,j)}$. We experimentally observed the convergence of the entropic method. Proof of global convergence of the block entropic projection method will be studied in the future.

III. An Application: Computer Vision Based Wildfire Detection

The Entropy function based Adaptive Decision Fusion (EADF) framework described in detail in the previous section with tracking capability is especially useful when the online active learning problem is of a dynamic nature with drifting concepts [35], [36], [37]. In the video based wildfire detection problem introduced in this section, the nature of forestal recordings vary over time due to weather conditions and changes in illumination, which makes it necessary to deploy an adaptive wildfire detection system. It is not feasible to develop one strong fusion model with fixed weights in this setting with drifting nature. An ideal online active learning mechanism should keep track of drifts in video and adapt itself accordingly. The projections in Eq. 12 and Eq. 4 adjust the importance of individual sub-algorithms by updating the weights according to the decisions of the oracle.

Manned lookout posts are widely available in forests all around the world to detect wildfires. Surveillance cameras can be placed in these surveillance towers to monitor the surrounding forestal area for possible wildfires. Furthermore, they can be used to monitor the progress of the fire from remote centers.

As an application of EADF, a computer vision based method for wildfire detection is presented in this article. Security guards have to work 24 hours in remote locations under difficult circumstances. They may simply get tired or leave the lookout tower for various reasons. Therefore, computer vision based video analysis systems capable of producing automatic fire alarms are necessary to help the security guards to reduce the average forest fire detection time.

Cameras, once installed, operate at forest watch towers throughout the fire season for about six months which is mostly dry and sunny in the Mediterranean region. There is usually a guard in charge of the cameras, as well. The guard can supply feed-back to the detection algorithm after the installation of the system. Whenever an alarm is issued, she/he can verify it or reject it. In this way, she/he can participate in the learning process of the adaptive algorithm. The proposed active fusion algorithm can also be used in other supervised learning problems where classifiers combinations through feedback is required.

As described in the following section, the main wildfire detection algorithm is composed of five sub-algorithms. Each algorithm has its own decision function yielding a zero-mean real number for slow moving regions at every image frame of a video sequence. Decision values from sub-algorithms are linearly combined and weights of sub-algorithms are adaptively updated in our approach.

There are several approaches on automatic forest fire detection in the literature. Some of the approaches are directed towards detection of the flames using infra-red and/or visible-range cameras and some others aim at detecting the smoke due to wildfire [38], [39], [40], [41], [42]. There are recent papers on sensor based fire detection [43], [44], [45]. Infrared cameras and sensor based systems have the ability to capture the rise in temperature, however, they are much more expensive compared to regular pan-tilt-zoom (PTZ) cameras. An intelligent space framework is described for indoor fire detection in [46]. However, in this paper, an outdoor (forest) wildfire detection method is proposed.

It is almost impossible to view flames of a wildfire from a camera mounted on a forest watch tower unless the fire is very near to the tower. However, smoke rising up in the forest due to a fire is usually visible from long distances. A snapshot of typical wildfire smoke captured by a lookout tower camera from a distance of 5 km is shown in Fig. 2.

Guillemant and Vicente [42] based their method on the observation that the movements of various patterns, like smoke plumes, produce correlated temporal segments of gray-level pixels. They utilized fractal indexing using a space-filling Z-curve concept along with instantaneous and cumulative velocity histograms for possible smoke regions. They made smoke decisions about the existence of smoke according to the standard deviation, minimum average energy, and the shape and smoothness of these histograms. It is possible to include most of the currently available methods as sub-algorithms in the proposed framework and combine their decisions using the proposed EADF method.

Smoke at far distances (> 100 m to the camera) exhibits different spatio-temporal characteristics than nearby smoke and fire [47], [48], [49]. This demands specific methods explicitly developed for smoke detection at far distances rather than using nearby smoke detection methods described in [50]. The proposed approach is in accordance with the ‘weak’ Artificial Intelligence (AI) framework [51] introduced by Hubert L. Dreyfus, as opposed to ‘generalized’ AI. According to this framework, each specific problem in AI should be addressed as an individual engineering problem with its own characteristics [52], [53].

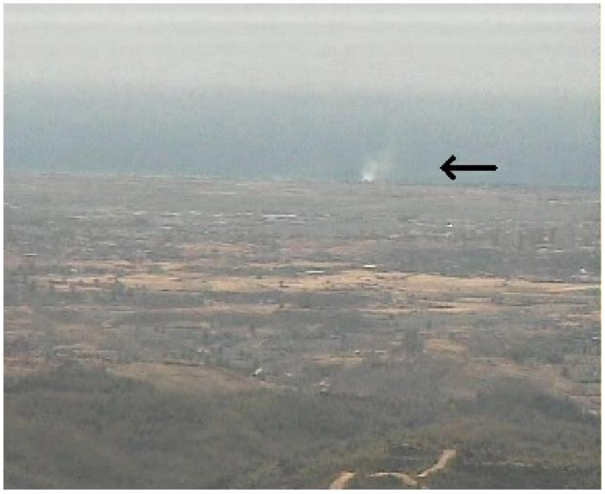

Fig. 2. Snapshot of typical wildfire smoke captured by a forest watch tower which is 5 km away from the fire (rising smoke is marked with an arrow).

IV. Building Blocks of Wildfire Detection Algorithm

Wildfire detection algorithm is developed to recognize the existence of wildfire smoke within the viewing range of the camera monitoring forestal areas. The proposed wildfire smoke detection algorithm consists of five main sub-algorithms: (i) slow moving object detection in video, (ii) smoke-colored region detection, (iii) wavelet transform based region smoothness detection, (iv) shadow detection and elimination, (v) covariance matrix based classification, with decision functions, $D_1(x,n)$, $D_2(x,n)$, $D_3(x,n)$, $D_4(x,n)$ and $D_5(x,n)$, respectively, for each pixel at location x of every incoming image frame at time step n. Computationally efficient sub-algorithms are selected in order to realize a real-time wildfire detection system working in a standard PC. The decision functions are combined in a linear manner and the weights are determined according to the weight update mechanism described in Section II.

Decision functions $D_i, \quad i = 1, ..., M$ of sub-algorithms do not produce binary values 1 (correct) or -1 (false), but they produce real numbers centered around zero for each incoming sample x. If the number is positive (negative), then the individual algorithm decides that there is (not) smoke due to forest fire in the viewing range of the camera. Output values of decision functions express the confidence level of each sub-algorithm. The higher the value, the more confident the algorithm.

The first four sub-algorithms are described in detail in [54] which is available online at the EURASIP webpage. We recently added the fifth sub-algorithm to our system. It is briefly reviewed below.

A. Covariance Matrix Based Region Classification

The fifth sub-algorithm deals with the classification of the smoke colored moving regions. We first obtain a mask from the intersection of the first two sub-algorithms and use the obtained smoke colored moving regions as the input to the fifth algorithm. The regions are passed as bounding boxes of the connected regions of the mask. A region covariance matrix [55] consisting of discriminative features is calculated for each region. For each pixel in the region, a 9-dimensional feature vector z_k is calculated as follows:

$$z_k = \Bigg[x_1 \; x_2 \; Y(x_1,x_2) \; U(x_1,x_2) \; V(x_1,x_2) \tag{23}$$

$$\left|\frac{dY(x_1,x_2)}{dx_1}\right| \; \left|\frac{dY(x_1,x_2)}{dx_2}\right| \; \left|\frac{d^2Y(x_1,x_2)}{dx_1^2}\right| \; \left|\frac{d^2Y(x_1,x_2)}{dx_2^2}\right| \Bigg]^T$$

where k is the label of a pixel, (x_1, x_2) is the location of the pixel, Y, U, V are the components of the representation of the pixel in YUV color space, $\frac{dY(x_1,x_2)}{dx_1}$ and $\frac{dY(x_1,x_2)}{dx_2}$ are the horizontal and vertical derivatives of the region respectively, calculated using the filter [-1 0 1], $\frac{d^2Y(x_1,x_2)}{dx_1^2}$ and $\frac{d^2Y(x_1,x_2)}{dx_2^2}$ are the horizontal and vertical second derivatives of the region calculated using the filter [-1 2 -1], respectively.

The feature vector for each pixel can be represented as follows:

$$z_k = [z_k(i)]^T \tag{24}$$

where, $z_k(i)$ is the i^{th} entry of the feature vector. This feature vector is used to calculate the 9 by 9 covariance matrix of the regions using the fast covariance matrix computation formula [56]:

$$C_R = [c_R(i,j)] = \left(\frac{1}{n-1} \left[\sum_{k=1}^{n} z_k(i) z_k(j) - Z_{kk} \right] \right) \tag{25}$$

where

$$Z_{kk} = \frac{1}{n} \sum_{k=1}^{n} z_k(i) \sum_{k=1}^{n} z_k(j)$$

where n is the total number of pixels in the region and $c_R(i,j)$ is the $(i,j)^{th}$ component of the covariance matrix.

The region covariance matrices are symmetric, therefore, we only need half of the elements of the matrix for classification. We also do not need the first 3 elements $c_R(1,1), c_R(2,1), c_R(2,2)$ when using the lower diagonal elements of the matrix, because these are the same for all regions. Then, we need a feature vector f_R with $9 \times 10/2 - 3 = 42$ elements for each region. For a given region, the final feature vector does not depend on the number of pixels in the region; it only depends on the number of features in z_k.

A Support Vector Machine (SVM) with RBF kernel is trained with the region covariance feature vectors of smoke regions in the training database. We used 18680 images used to train the SVM. The number of positive images which have actual smoke is 7011, and the rest are negative images that do not have smoke. Sample positive and negative images are shown in Fig. 3. The confusion matrix for the training set is given in Table I. The success rate is 99.3% for the positive images and 97.2% for the negative images.

TABLE I
CONFUSION MATRIX OF THE TRAINING SET

		Predicted Labels	
		Not Smoke	Smoke
Actual	Not Smoke	11342/(97.2)%	327/ (3.8%)
Labels	Smoke	49/ (0.7%)	6962/(99.3%)

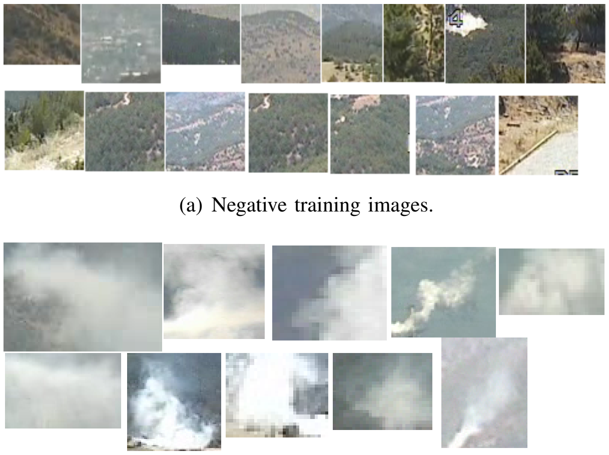

(a) Negative training images.

(b) Positive training images

Fig. 3. Positive and negative images from the training set.

The LIBSVM [57] software library is used to obtain the posterior class probabilities, $p_R = Pr(label = 1|f_R)$, where $label = 1$ corresponds to a smoke region. In this software library, posterior class probabilities are estimated by approximating the posteriors with a sigmoid function as in [58]. If the posterior probability is larger than 0.5, the label is 1 and the region contains smoke according to the covariance descriptor. The decision function for this sub-algorithm is defined as follows:

$$D_5(x,n) = 2p_R - 1 \tag{26}$$

where $0 < p_R < 1$ is the estimated posterior probability that the region contains smoke. In [55], a distance measure based on eigenvalues are used to compare covariance matrices, but we found that individual covariance values also provide satisfactory results in this problem.

As pointed out above, the decision results of five sub-algorithms, D_1, D_2, D_3, D_4 and D_5, are linearly combined to reach a final decision on a given pixel; whether it is a pixel of a smoke region or not. Morphological operations are applied to the detected pixels to mark the smoke regions. The number of connected smoke pixels should be larger than a threshold to issue an alarm for the region. If a false alarm is issued during the training phase, the oracle gives feedback to the algorithm by declaring a no-smoke decision value ($y = -1$) for the false alarm region. Initially, equal weights are assigned to each sub-algorithm. There may be large variations between forestal areas and substantial temporal changes may occur within the same forestal region. As a result, weights of individual sub-algorithms will evolve in a dynamic manner over time.

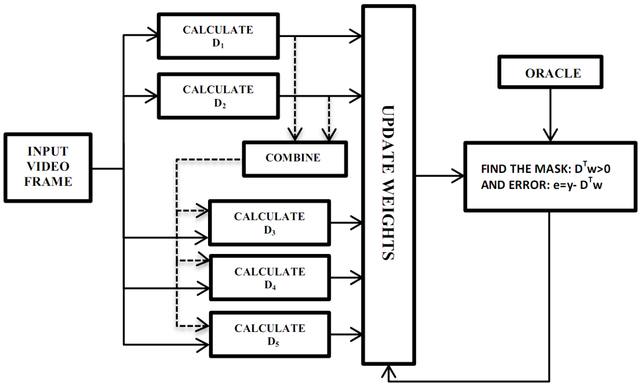

Fig. 4. Flowchart of the weight update algorithm for one image frame.

In real-time operating mode the PTZ cameras are in continuous scan mode visiting predefined preset locations. In this mode, constant monitoring from the oracle can be relaxed by adjusting the weights for each preset once, and then use the same weights for successive classifications. Since the main issue is to reduce false alarms, the weights can be updated when there is no smoke in the viewing range of each preset and after that, the system becomes autonomous. The cameras stop at each preset and run the detection algorithm for some time before moving to the next preset. By calculating separate weights for each preset, we are able to reduce false alarms.

V. Experimental Results

A. Experiments on wildfire detection

The proposed wildfire detection scheme with entropy functional based active learning method is implemented on a PC with an Intel Core Duo CPU 2.6GHz processor and tested with forest surveillance recordings captured from cameras mounted on top of forest watch towers near Antalya and Mugla provinces in Mediterranean region in Turkey. The weather is stable with sunny days throughout the entire summer in Mediterranean. If it happens to rain there is no possibility of forest fire. *The installed system successfully detected three forest fires in the summer of 2008*. The system was also independently tested by the Regional Technology Clearing House of San Diego State University in California in April 2009, and it detected the test fire and did not produce any false alarms during the trials. A snapshot from this test is presented in Fig. 5. The system also detected another forest fire in Cyprus in 2010. The software is currently being used in more than 60 forest watch towers in Turkey, Greece and Cyprus.

The proposed EADF strategy is compared with the universal linear predictor (ULP) scheme proposed by Singer and Feder [59]. The ULP adaptive filtering method is modified to the wildfire detection problem in an online learning framework. In the ULP scheme, decisions of individual algorithms are linearly combined, similar to Eq. 1 as follows:

$$\hat{y}_u(x,n) = \sum_i v_i(n) D_i(x,n) \tag{27}$$

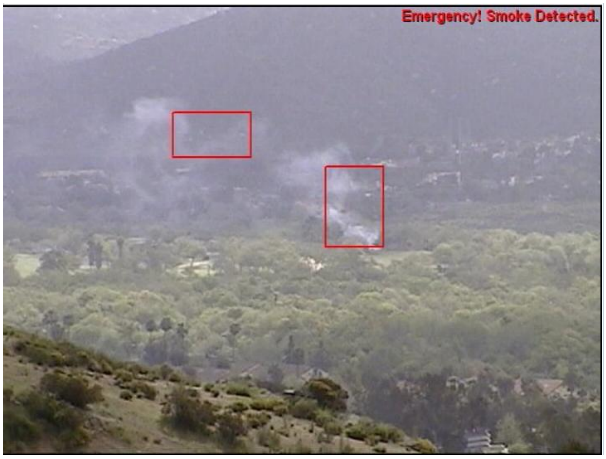

Fig. 5. A snapshot from an independent test of the system by the Regional Technology Clearing House of San Diego State University in California in April 2009. The system successfully detected the test fire and did not produce any false alarms. The detected smoke regions are marked with rectangles.

where the weights, $v_i(n)$, are updated according to the ULP algorithm, which assumes that the data (or decision values $D_i(x,n)$, in our case) are governed by some unknown probabilistic model P [59]. The objective of a universal predictor is to minimize the expected cumulative loss. An explicit description of the weights, $v_i(n)$, of the ULP algorithm is given as follows:

$$v_i(n+1) = \frac{exp(-\frac{1}{2c}\ell(y(x,n), D_i(x,n)))}{\sum_j exp(-\frac{1}{2c}\ell(y(x,n), D_j(x,n)))} \tag{28}$$

where c is a normalization constant and the loss function for the i-th decision function is:

$$\ell(y(x,n), D_i(x,n)) = [y(x,n) - D_i(x,n)]^2 \tag{29}$$

The constant c is taken as 4 as indicated in [59]. The universal predictor based algorithm is summarized in Algorithm 3.

Algorithm 3 The pseudo-code for the universal predictor

```
Universal Predictor(x,n)
for $i$ = 1 to M do
    $\ell(y(x,n), D_i(x,n)) = [y(x,n) - D_i(x,n)]^2$
    $v_i(n+1) = \frac{exp(-\frac{1}{2c}\ell(y(x,n),D_i(x,n)))}{\sum_j exp(-\frac{1}{2c}\ell(y(x,n),D_j(x,n)))}$
end for
$\hat{y}_u(x,n) = \sum_i v_i(n) D_i(x,n)$
if $\hat{y}_u(x,n) \geq 0$ then
    return 1
else
    return -1
end if
```

In the experiments, we compared eight different algorithms named FIXED, ULP, NLMS, NLMS-B, EADF, EADF-B, LOGX and LOG(X+1). NLMS-B and EADF-B are block projection versions of NLMS and EADF based methods with block size $q = 5$. LOGX and LOG(X+1) represent the algorithms that use $-logx$ and $-log(x+1)$ as the distance functions. FIXED represents the unadaptive method that uses fixed weights and ULP is the universal linear predictor based approach. In Tables II, IV and V, forest surveillance recordings containing actual forest fires and test fires, as well as, video sequences with no fires are used.

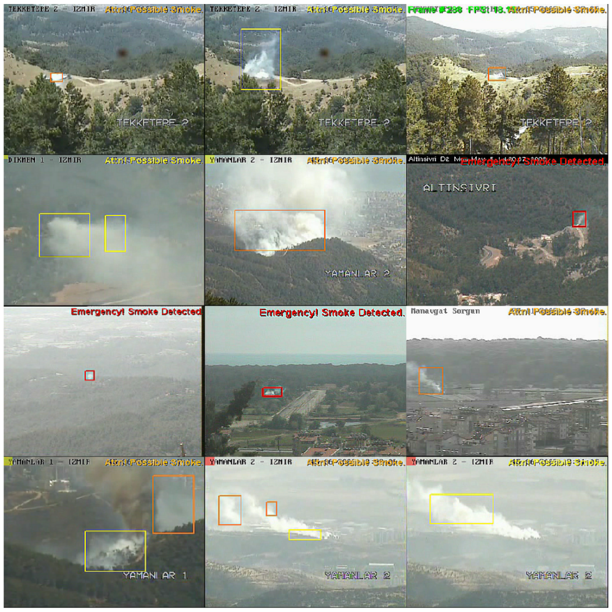

Fig. 6. Snapshots from the test videos in Table II. The first two and the last two images are from the same video sequences.

In Table II, 10 video sequences that contain wildfire smoke are tested in terms of true detection rates, which is defined as the number of correctly classified frames containing smoke divided by the total number of frames which contain smoke. $V2$, $V4$, $V5$ and $V10$ contain actual forest fires recorded by the cameras at forest watch towers, and the others contain artificial test fires. FIXED and ULP methods usually have higher detection rates but there is not a significant difference from the adaptive methods. Our aim is to decrease false alarms without reducing the detection rates too much. Table IV is generated from the first alarm frames and times of the algorithms. The times are comparable to each other and all algorithms produced alarms in less than 13 seconds. Snapshots from the test results in Table II are given in Fig. 6. For the wildfire detection problem another important comparison criteria is false negative (miss) detection rate, which is defined as the number of incorrectly classified frames containing smoke divided by the total number of frames which contain smoke. In Table III, the video sequences that contain wildfire smoke are tested in terms of false negative (miss) detection rates.

A set of video clips containing clouds, moving cloud shadows, fog and other moving regions that usually cause false alarms is used to generate Table V. The algorithms are compared in terms of false alarm rates, which is defined as the number of misclassified frames that do not contain smoke, divided by the total number of frames that do not contain smoke. Except for one video sequence, EADF method produces the lowest false alarm rate in the dataset. The algorithms that use adaptive fusion strategy significantly reduce the false alarm rate of the system compared to the non-adaptive methods by integrating the feedback from the guard (oracle) into the decision mechanism within the active learning framework. One interesting result is that EADF-B and NLMS-B, which are the versions that use the block projection method developed for the case of infinite number of convex sets, usually produced more false alarms than the methods that do not use block projections.

In Fig. 7 typical false alarms issued to videos by an untrained algorithm with decision weights equal to $\frac{1}{5}$ are shown.

In Fig. 8, the squared pixels errors of NLMS and EADF based schemes are compared for the video clip $V12$. The average pixel error for a video sequence v is calculated as follows:

$$\bar{E}(v) = \frac{1}{F_I}\sum_{n=1}^{F_I}(\frac{e_n}{N_I}) \qquad (30)$$

where N_I is the total number of pixels in the image frame, F_I is the number of frames in the video sequence, and e_n is the sum of the squared errors for each classified pixel in

TABLE II

EIGHT DIFFERENT ALGORITHMS ARE COMPARED IN TERMS OF TRUE DETECTION RATES IN VIDEO CLIPS THAT CONTAIN WILDFIRE SMOKE.

		True Detection Rates							
Video	Frames	FIXED	ULP	NLMS	NLMS-B	EADF	EADF-B	LOGX	LOG(X+1)
V1	768	87.63%	87.63%	87.63%	87.63%	87.63%	87.63%	87.89%	87.63%
V2	300	89.67%	**89.67**%	83.00%	89.66%	81.33%	86.00%	84.67%	89.66%
V3	550	**70.36**%	**70.36**%	68.18%	68.18%	67.09%	68.18%	67.09%	68.00%
V4	1000	**94.90**%	**94.90**%	90.80%	94.10%	90.50%	92.40%	93.30%	93.70%
V5	1000	**96.30**%	95.50%	91.10%	92.90%	91.90%	92.70%	92.40%	93.40%
V6	439	**80.87**%	**80.87**%	80.41%	80.41%	80.41%	80.41%	80.41%	80.41%
V7	770	85.71%	85.71%	85.71%	85.71%	85.84%	85.71%	85.71%	**85.97**%
V8	1060	98.68%	**99.15**%	98.86%	98.68%	98.77%	98.67%	98.96%	98.77%
V9	410	**80.24**%	**80.24**%	80.00%	80.00%	80.00%	80.00%	80.00%	80.00%
V10	1000	82.30%	82.30%	79.30%	82.40%	89.50%	90.70%	**91.10**%	81.30%
Avg.	-	**86.67**%	86.63%	84.50%	85.97%	85.30%	86.24%	86.15%	85.88

TABLE III

EIGHT DIFFERENT ALGORITHMS ARE COMPARED IN TERMS OF FALSE NEGATIVE (MISS) DETECTION RATES IN VIDEO CLIPS THAT CONTAIN WILDFIRE SMOKE.

		Miss Detection Rates							
Video	Frames	FIXED	ULP	NLMS	NLMS-B	EADF	EADF-B	LOGX	LOG(X+1)
V1	768	12.37%	12.37%	12.37%	12.37%	12.37%	12.37%	12.11%	12.37%
V2	300	10.33%	**10.33**%	17.00%	10.34%	18.67%	14.00%	15.33%	10.34%
V3	550	**29.64**%	**29.64**%	31.82%	31.81%	32.91%	31.82%	32.91%	32.00%
V4	1000	**5.10**%	**5.10**%	9.20%	5.90%	9.50%	7.60%	6.70%	6.30%
V5	1000	**3.70**%	4.50%	8.90%	7.10%	8.10%	7.30%	7.60%	6.60%
V6	439	**9.13**%	**9.13**%	9.59%	9.59%	9.59%	9.59%	9.59%	9.59%
V7	770	4.29%	4.29%	4.29%	4.29%	4.16%	4.29%	4.29%	**4.03**%
V8	1060	1.32%	**0.85**%	1.14%	1.32%	1.23%	1.33%	1.04%	1.23%
V9	410	**19.76**%	**19.76**%	20.00%	20.00%	20.00%	20.00%	20.00%	20.00%
V10	1000	17.70%	17.70%	20.70%	17.60%	20.50%	19.30%	**8.90**%	18.70%
Average	-	**13.33**%	13.37%	15.50%	14.03%	14.70%	13.76%	13.85%	14.12

TABLE IV

EIGHT DIFFERENT ALGORITHMS ARE COMPARED IN TERMS OF FIRST ALARM FRAMES AND TIMES IN VIDEO CLIPS THAT CONTAIN WILDFIRE SMOKE.

	First Alarm Frame / Time (secs.)							
Video	FIXED	ULP	NLMS	NLMS-B	EADF	EADF-B	LOGX	LOG(X+1)
V1	64/12.80	64/12.80	64/12.80	64/12.80	64/12.80	64/12.80	64/12.80	64/12.80
V2	42/8.40	42/8.40	67/13.40	42/8.40	68/13.60	53/10.60	58/11.60	42/8.40
V3	26/5.20	26/5.20	37/7.40	37/7.40	44/8.80	37/7.40	43/8.60	38/7.60
V4	25/5.00	25/5.00	58/11.60	25/5.00	59/11.80	33/6.60	25/5.00	43/8.60
V5	32/6.40	35/7.00	53/10.60	35/7.00	54/10.80	35/7.00	35/7.00	36/7.20
V6	21/4.20	21/4.20	21/4.20	21/4.20	21/4.20	21/4.20	21/4.20	21/4.20
V7	47/1.88	47/1.88	47/1.88	47/1.88	47/1.88	47/1.88	47/1.88	47/1.88
V8	12/1.33	12/1.33	12/1.33	12/1.33	12/1.33	12/1.33	12/1.33	12/1.33
V9	67/2.68	67/2.68	67/2.68	67/2.68	67/2.68	67/2.68	67/2.68	67/2.68
V10	33/6.60	33/6.60	50/10.00	33/6.60	51/10.20	33/6.60	33/6.60	44/8.80
Avg.	36.90/5.45	37.20/5.51	47.60/7.59	38.30/5.73	48.70/7.81	40.20/6.11	40.50/6.17	41.40/6.35

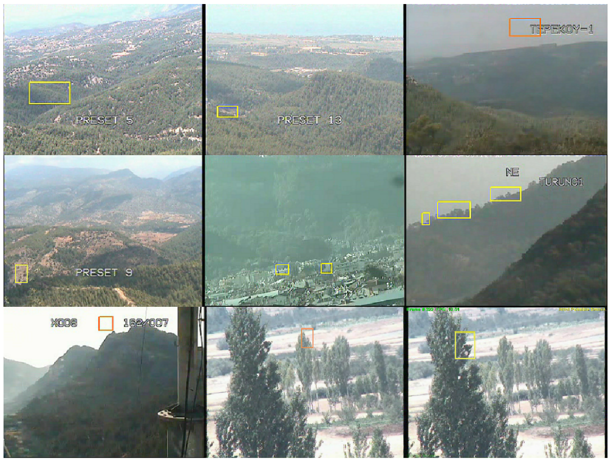

Fig. 7. False alarms issued to videos from Table V. The first two and the last two images are from the same video sequences. Cloud shadows, clouds, fog, moving tree leaves, and sunlight reflecting from buildings cause false alarms in an untrained algorithm with decision weights equal to $\frac{1}{5}$.

TABLE V
EIGHT DIFFERENT ALGORITHMS ARE COMPARED IN TERMS OF FALSE ALARM RATES IN VIDEO CLIPS THAT DO NOT HAVE WILDFIRE SMOKE.

		False Alarm Rates							
Video	Frames	FIXED	ULP	NLMS	NLMS-B	EADF	EADF-B	LOGX	LOG(X+1)
V11	6300	0.03%	0.03%	0.03%	0.03%	**0.02**%	0.03%	0.03%	0.03%
V12	3370	7.00%	2.97%	1.01%	1.96%	**0.92**%	1.01%	1.66%	0.89%
V13	7500	3.13%	3.12%	2.77%	2.77%	2.77%	2.77%	**2.24**%	2.77%
V14	6294	17.25%	9.64%	2.27%	2.67%	**2.18**%	2.40%	3.23%	4.89%
V15	6100	4.33%	4.21%	2.72%	2.75%	1.80%	2.75%	**1.23**%	2.97%
V16	433	11.32%	11.32%	0.00%	0.00%	**0.00**%	0.00%	0.00%	0.00%
V17	7500	0.99%	0.00%	0.00%	0.00%	**0.00**%	0.00%	0.00%	0.00%
Average	-	6.29%	4.47%	1.26%	1.46%	**1.10**%	1.28%	1.20%	1.65%

image frame n. The figure shows the average errors for the frames between 500 and 900 of $V12$. At around the frames 510 and 800, the camera moves to a new position and weights are reset to their initial values. The EADF algorithm achieves convergence faster than the NLMS algorithm. The tracking performance of the EADF algorithm is also better than the NLMS based algorithm which can be observed after the frame number 600, at which point some of the sub-algorithms issue false alarms.

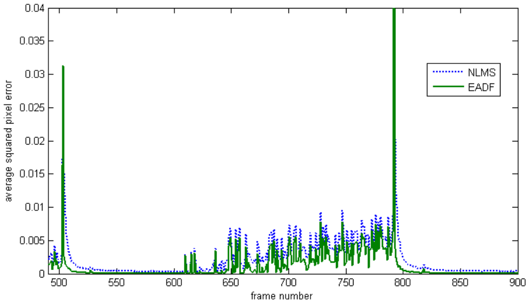

Fig. 8. Average squared pixel errors for the NLMS and the EADF based algorithms for the video seuqence $V12$.

In Fig. 9 the weights of two different pixels from $V12$ are displayed for 140 frames. For the first pixel, $D_1(x,n)$, $D_3(x,n)$ and $D_4(x,n)$ get closer to 1 after the 60^{th} frame, and therefore, their weights are reduced. For the second pixel, $D_2(x,n)$ issues false alarms after the 4^{th} frame; $D_2(x,n)$ and $D_4(x,n)$ issue false alarms after the 60^{th} frame.

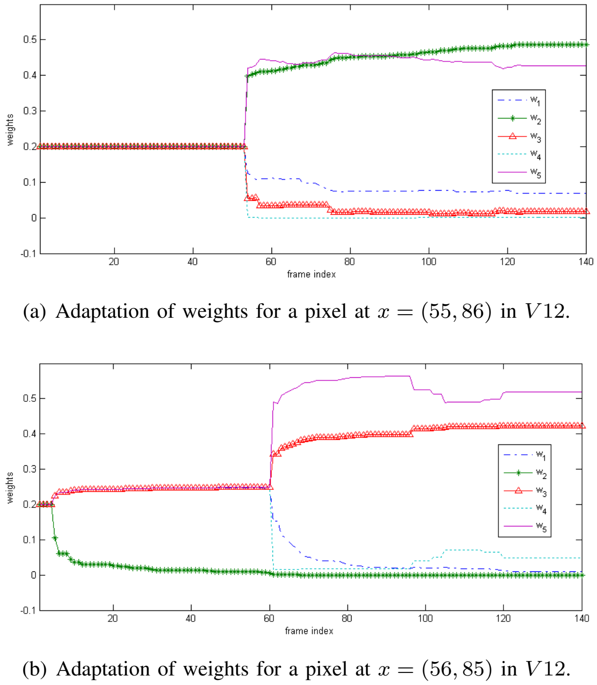

(a) Adaptation of weights for a pixel at $x = (55, 86)$ in $V12$.

(b) Adaptation of weights for a pixel at $x = (56, 85)$ in $V12$.

Fig. 9. Adaptation of weights in a video that do not contain smoke.

B. Experiments on a UCI Dataset

The proposed method is also tested with a dataset from the UCI (University of California, Irvine) machine learning repository to evaluate the performance of the algorithm in combining different classifiers. In the wildfire detection case, the image data arrives sequentially and the decision weights are updated in real-time. On the other hand, the UCI data sets are fixed. Therefore the dataset is divided into two parts: training and testing.

During the training phase, weights of different classifiers are determined using the EADF update method. In the testing phase, the fixed weights obtained from the training phase are used to combine the classifier decisions, which process the data in a sequential manner because both the NLMS and the EADF frameworks assume that the new data arrive in a sequential manner.

The test is performed on the ionosphere data from the UCI machine learning repository that consists of radar measurements to detect the existence of free electrons that form a structure in the atmosphere. The electrons that show some kind of structure in the ionosphere return "Good" responses; the others return "Bad" responses. There are 351 samples with 34-element feature vectors that are obtained by passing the radar signals through an autocorrelation function. In [60], the first 200 samples are used as the training set to classify the remaining 151 test samples. They obtained 90.7% accuracy with a linear perceptron, 92% accuracy with a non-linear perceptron, and 96% accuracy with a back propagation neural network.

For this test, SVM, k-nn (k-Nearest Neighbor) and NCC (normalized cross-correlation) classifiers are used. Also, in this classification the decision functions of these classifiers produce binary values with 1 corresponding to “Good” classification and -1 corresponding to “Bad” classification rather than scaled posterior probabilities in the range $[-1, 1]$.

The accuracies of the sub-algorithms and EADF are shown in Table VI. The success rates of the proposed EADF and NLMS methods are both 98.01% which is higher than all the sub-algorithms. Both the entropic projection and orthogonal projection based algorithms converge to a solution in the intersection of the convex sets. It turns out that they both converge to the same solution in this particular case. This is possible when the intersection set of convex sets is small. The proposed EADF method is actually developed for real-time application in which data arrives sequentially. This example is included to show that the EADF scheme can also be used in other datasets. It may be possible to get better classification results with other classifiers in this fixed UCI dataset.

TABLE VI
ACCURACIES OF SUB-ALGORITHMS AND EADF ON IONOSPHERE DATASET.

Data	Success Rates (%)				
	SVM	k-nn (k=4)	NCC	NLMS	EADF
Train	100.0	91.50	100.0	100.0	100.0
Test	94.03	97.35	91.39	98.01	98.01

VI. CONCLUSION

An entropy functional based online adaptive decision fusion (EADF) is proposed for image analysis and computer vision applications with drifting concepts. In this framework, it is assumed that the main algorithm for a specific application is composed of several sub-algorithms each of which yields its own decision as a real number centered around zero, representing its confidence level. Decision values are linearly combined with weights which are updated online by performing non-orthogonal e-projections onto convex sets describing sub-algorithms. This general framework is applied to a real computer vision problem of wildfire detection. The proposed adaptive decision fusion strategy takes into account the feedback from guards of forest watch towers. Experimental results show that the learning duration is decreased with the proposed online adaptive fusion scheme. It is also observed that error rate of the proposed method is the lowest in our data set, compared to the universal linear predictor (ULP) and the normalized least mean square (NLMS) based schemes.

The proposed framework for decision fusion is suitable for problems with concept drift. At each stage of the algorithm, the method tracks the changes in the nature of the problem by performing an non-orthogonal e-projection onto a hyperplane describing the decision of the oracle.

ACKNOWLEDGMENT

This work was supported in part by the Scientific and Technical Research Council of Turkey, TUBITAK, with grant no. 106G126 and 105E191, in part by European Commission 6th Framework Program with grant number FP6-507752 (MUSCLE Network of Excellence Project) and in part by FIRESENSE (Fire Detection and Management through a Multi-Sensor Network for the Protection of Cultural Heritage Areas from the Risk of Fire and Extreme Weather Conditions, FP7-ENV-2009-1244088-FIRESENSE) .

REFERENCES

[1] O. Günay, K. Taşdemir, B. U. Töreyin, and A. E. Çetin, “Video based wildfire detection at night,” *Fire Safety Journal*, vol. 44, no. 6, pp. 860–868, 2009.

[2] S. Theodoridis, K. Slavakis, and I. Yamada, “Adaptive Learning in a World of Projections,” *IEEE Signal Processing Magazine*, vol. 28, no. 1, pp. 97–123, 2011.

[3] T. K. Ho, J.J. Hull, and S.N. Srihari, “Decision combination in multiple classifier systems,” *IEEE Transactions on Pattern Analysis and Machine Intelligence*, vol. 16, no. 1, pp. 66–75, 1994.

[4] V. I. Gorodetskiy and S. V. Serebryakov, “Methods and algorithms of collective recognition,” *Automation and Remote Control*, vol. 69, no. 11, pp. 1821–1851, 2008.

[5] B.V. Dasarathy and B.V. Sheela, “A composite classifier system design: Concepts and methodology,” *Proceedings of the IEEE*, vol. 67, no. 5, pp. 708–713, 1979.

[6] A. Kumar and D. Zhang, “Personal authentication using multiple palmprint representation,” *Pattern Recognition*, vol. 38, no. 10, pp. 1695–1704, 2005.

[7] X. Tang and Z. Li, “Video based face recognition using multiple classifiers,” in *IEEE International Conference on Automatic Face and Gesture Recognition*, 2004, pp. 345–349.

[8] M. A. Garca and D. Puig, “Supervised texture classification by integration of multiple texture methods and evaluation windows,” *Image and Vision Computing*, vol. 25, no. 7, pp. 1091–1106, 2007.

[9] A. Frank and A. Asuncion, “UCI Machine Learning Repository,” http://archive.ics.uci.edu/ml, 2010, University of California, Irvine, School of Information and Computer Sciences.

[10] L. Xu, A. Krzyzak, and C.Y. Suen, “Methods of Combining Multiple Classifiers and Their Applications to Handwriting Recognition,” *IEEE Transactions on Systems, Man, and Cybernetics, Part B*, vol. 22, no. 3, pp. 418–435, 1992.

[11] L. I. Kuncheva, “Switching between selection and fusion in combining classifiers: an experiment,” *IEEE Transactions on Systems, Man, and Cybernetics, Part B*, vol. 32, no. 2, pp. 146–156, 2002.

[12] D. Parikh and R. Polikar, “An Ensemble-Based Incremental Learning Approach to Data Fusion,” *IEEE Transactions on Systems, Man, and Cybernetics, Part B*, vol. 37, no. 2, pp. 437–450, 2007.

[13] B. Widrow, J.M. McCool, M.G. Larimore, and Jr. Johnson, C.R., “Stationary and nonstationary learning characteristics of the LMS adaptive filter,” *Proceedings of the IEEE*, vol. 64, no. 8, pp. 1151–1162, 1976.

[14] L. G. Gubin, B. T. Polyak, and E. V. Raik, “The method of projections for finding the common point of convex sets,” *USSR Computational Mathematics and Mathematical Physics*, vol. 7, no. 6, pp. 1 – 24, 1967.

[15] D. C. Youla and H. Webb, “Image restoration by the method of convex projections, Part I-Theory,” *IEEE Transactions on Medical Imaging*, vol. MI-I-2, pp. 81–94, 1982.

[16] A. E. Çetin, “Reconstruction of signals from Fourier transform samples,” *Signal Processing*, vol. 16, pp. 129–148, 1989.

[17] K. Slavakis, S. Theodoridis, and I. Yamada, “Online Kernel-Based Classification Using Adaptive Projection Algorithms,” *IEEE Transactions on Signal Processing*, vol. 56, pp. 2781–2796, 2008.

[18] U. Niesen, D. Shah, and G. Wornell, “Adaptive Alternating Minimization Algorithms,” *IEEE Transactions on Information Theory*, vol. 55, no. 3, pp. 1423–1429, 2009.

[19] I. Yamada and N. Ogura, “Adaptive Projected Subgradient Method for Asymptotic Minimization of Sequence of Nonnegative Convex Functions,” *Numerical Functional Analysis and Optimization*, vol. 25, no. 7, pp. 593–617, 2005.

[20] K. Slavakis, Yamada I., and Ogura N., “The adaptive projected subgradient method over the fixed point set of strongly attracting nonexpansive mappings,” *Numerical functional analysis and optimization*, vol. 27, no. 7, pp. 905–930, 2006.

[21] A. E. Çetin and R. Ansari, “Signal recovery from wavelet transform maxima,” *IEEE Transactions on Signal Processing*, vol. 42-1, pp. 194–196, 1994.

[22] P.L. Combettes, "The foundations of set theoretic estimation," *Proceedings of the IEEE*, vol. 81, no. 2, pp. 182–208, 1993.

[23] S. Theodoridis and M. Mavroforakis, "Reduced Convex Hulls: A Geometric Approach to Support Vector Machines," *IEEE Signal Processing Magazine*, vol. 24, pp. 119–122, 2007.

[24] S. Theodoridis and K. Koutroumbas, *Pattern Recognition*, Academic Press, 2006.

[25] G. Baraniuk, "Compressed sensing [Lecture Notes]," *IEEE Signal Processing Magazine*, vol. 24, no. 4, pp. 118–124, 2007.

[26] E. J. Candes, J. Romberg, and T. Tao, "Robust uncertainty principles: exact signal reconstruction from highly incomplete frequency information," *IEEE Transactions on Information Theory*, vol. 52, no. 2, pp. 489–509, 2006.

[27] J.-F. Cai, S. Osher, and Z. Shen, "Fast Linearized Bregman Iteration for Compressed Sensing," in *UCLA CAM Reports*, 2008, pp. 08–37.

[28] J.-F. Cai, S. Osher, and Z. Shen, "Linearized Bregman iterations for Compressed Sensing," *Mathematics of Computation*, vol. 78, no. 267, pp. 1515–1536, 2009.

[29] L. M. Bregman, "The Relaxation Method of Finding the Common Point of Convex Sets and Its Application to the Solution of Problems in Convex Programming," *USSR Computational Mathematics and Mathematical Physics*, vol. 7, pp. 200–217, 1967.

[30] G. T. Herman, "Image Reconstruction From Projections," *Real-Time Imaging*, vol. 1, no. 1, pp. 3–18, 1995.

[31] Y. Censor and A. Lent, "An iterative row-action method for interval convex programming," *Journal of Optimization theory and Applications*, vol. 34, no. 3, pp. 321–353, 1981.

[32] H.J. Trussell and M. R. Civanlar, "The Landweber iteration and projection onto convex set," *IEEE Transactions on Acoustics, Speech and Signal Processing*, vol. 33, no. 6, pp. 1632–1634, 1985.

[33] M.I. Sezan and H. Stark, "Image Restoration by the Method of Convex Projections: Part 2-Applications and Numerical Results," *IEEE Transactions on Medical Imaging*, vol. 1, no. 2, pp. 95–101, 1982.

[34] Y. Censor and A. Lent, "Optimization of "log x" entropy over linear equality constraints," *SIAM Journal on Control and Optimization*, vol. 25, pp. 921–933, 1987.

[35] J. C. Schlimmer and R. H. Granger, "Incremental learning from noisy data," *Machine Learning*, vol. 1, no. 3, pp. 317–354, 1986.

[36] M. Karnick, M. Ahiskali, M.D. Muhlbaier, and R. Polikar, "Learning concept drift in nonstationary environments using an ensemble of classifiers based approach," in *IEEE International Joint Conference on Neural Networks (IJCNN)*, 2008, pp. 3455–3462.

[37] K. Nishida, S. Shimada, S. Ishikawa, and K. Yamauchi, "Detecting sudden concept drift with knowledge of human behavior," in *IEEE International Conference on Systems, Man and Cybernetics*, 2008, pp. 3261–3267.

[38] J. R. Martinez-de Dios, B. C. Arrue, A. Ollero, L. Merino, and F. Gómez-Rodríguez, "Computer vision techniques for forest fire perception," *Image and Vision Computing*, vol. 26, pp. 550–562, 2008.

[39] J. Li, Q. Qi, X. Zou, H. Peng, L. Jiang, and Y. Liang, "Technique for Automatic Forest Fire Surveillance Using Visible Light Image," in *International Geoscience and Remote Sensing Symposium*, 2005, vol. 5, pp. 31–35.

[40] I. Bosch, S. Gomez, L. Vergara, and J. Moragues, "Infrared image processing and its application to forest fire surveillance," in *IEEE Conference on Advanced Video and Signal Based Surveillance (AVSS)*, 2007, pp. 283–288.

[41] T. Celik, H. Ozkaramanli, and H. Demirel, "Fire and Smoke Detection without Sensors: Image Processing Based Approach," in *European Signal Processing Conference (EUSIPCO)*, 2007, pp. 1794–1798.

[42] P. Guillemant and J. Vicente, "Real-time identification of smoke images by clustering motions on a fractal curve with a temporal embedding method," *Optical Engineering*, vol. 40, no. 4, pp. 554–563, 2001.

[43] M. Hefeeda and M. Bagheri, "Forest Fire Modeling and Early Detection using Wireless Sensor Networks," in *Proceedings of the IEEE International Conference on Mobile Adhoc and Sensor Systems (MASS)*, 2007, pp. 1–6.

[44] Y.G. Sahin, "Animals as Mobile Biological Sensors for Forest Fire Detection," *Sensors*, vol. 7, no. 12, pp. 3084–3099, 2007.

[45] S. Chen, H. Bao, X. Zeng, and Y. Yang, "A fire detecting method based on multi-sensor data fusion," in *IEEE International Conference on Systems, Man and Cybernetics*, 2003, vol. 4, pp. 3775–3780.

[46] P. Podrzaj and H. Hashimoto, "Intelligent Space as a Fire Detection System," in *IEEE International Conference on Systems, Man and Cybernetics*, 2006, pp. 2240–2244.

[47] B. U. Töreyin, Y. Dedeoğlu, and A. E. Çetin, "Flame Detection in Video Using Hidden Markov Models," in *International conference on Image Processing (ICIP)*, 2005, pp. 1230–1233.

[48] Y. Dedeoğlu, B. U. Töreyin, U. Güdükbay, and A. E. Çetin, "Real-time Fire and Flame Detection in Video," in *International Conference on Acoustics Speech and Signal Processing (ICASSP)*, 2005, pp. 669–672.

[49] B. U. Töreyin, Y. Dedeoğlu, U. Güdükbay, and A. E. Çetin, "Computer Vision Based System for Real-time Fire and Flame Detection," *Pattern Recognition Letters*, vol. 27, pp. 49–58, 2006.

[50] B. U. Töreyin, Y. Dedeoğlu, and A. E. Çetin, "Wavelet Based Real-Time Smoke Detection in Video," in *European Signal Processing Conference (EUSIPCO)*, 2005.

[51] T. Pavlidis, "Computers vs Humans," *http://www.theopavlidis.com/comphumans/ comphuman.htm*, 2002.

[52] H.L. Dreyfus, *What Computers Can't Do*, MIT Press, 1972.

[53] H.L. Dreyfus, *What Computers Still Can't Do*, MIT Press, 1992.

[54] B. U. Töreyin, *Fire Detection Algorithms Using Multimodal Signal and Image Analysis*, Ph.D. thesis, Bilkent University, 2009, http://www.arehna.di.uoa.gr/thesis/uploaded_data/Fire_Detection_Algorithms_Using_Multimodal_Signal_and_Image_Analysis_2009_thesis_1232106137.pdf.

[55] O. Tuzel, F. Porikli, and P. Meer, "Region Covariance: A Fast Descriptor for Detection And Classification," in *European Conference on Computer Vision (ECCV)*, 2006, pp. 589–600.

[56] F. Porikli and O. Tuzel, "Fast construction of covariance matrices for arbitrary size image windows," in *International Conference on Image Processing (ICIP)*, 2006, pp. 1581–1584.

[57] C.-C. Chang and C.-J. Lin, *LIBSVM: a library for support vector machines*, 2001, Software available at http://www.csie.ntu.edu.tw/~cjlin/libsvm.

[58] J. C. Platt, "Probabilistic Outputs for Support Vector Machines and Comparisons to Regularized Likelihood Methods," in *Advances in Large Margin Classifiers*. 1999, pp. 61–74, MIT Press.

[59] A. C. Singer and M. Feder, "Universal linear prediction by model order weighting," *IEEE Transactions on Signal Processing*, vol. 47-10, pp. 2685–2699, 1999.

[60] V. G. Sigillito, S. P. Wing, L. V. Hutton, and K. B. Baker, "Classification of radar returns from the ionosphere using neural networks," *Johns Hopkins APL Technical Digest*, pp. 262–266, 1989.

Osman Günay received his B.Sc. and M.S. degrees in Electrical and Electronics Engineering from Bilkent University, Ankara, Turkey. Since 2009, he has been a Ph.D. Student in the Department of Electrical and Electronics Engineering at Bilkent University, Ankara, Turkey. His research interests include computer vision, video segmentation, and dynamic texture recognition.

Behçet Uğur Töreyin received his PhD and MS degrees from Bilkent University and BS degree from Middle East Technical University, Ankara, Trkiye, all in electrical and electronics engineering. Between 2009 and 2011, he was a postdoctoral research associate at the Robotic Sensor Networks Lab, University of Minnesota, Minnesota and at the Wireless Research Lab, Texas A&M University at Qatar, respectively. He is now an assistant professor at Cankaya University, Ankara, Turkey.

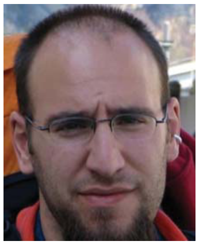

Kıvanç Köse is currently working through his PhD degree at the Electrical and Electronics Engineering Department at Bilkent. He studied the compression of the 3D mesh models during his MSc period under the supervision of Professor Enis Cetin. He implemented a new orthographic projection method for 3D model. Moreover, he implemented a new adaptive wavelet transformation called connectivity guided adaptive wavelet transformation, for this projected 2D model. He has experience on adaptive wavelet transformation and its applications in image processing.

A. Enis Çetin got his Ph.D. degree from the University of Pennsylvania in 1987. Between 1987-1989, he was Assistant Professor of Electrical Engineering at the University of Toronto. He has been with Bilkent University, Ankara, Turkey, since 1989. A.E. Cetin was an Associate Editor of the IEEE Trans. on Image Processing between 1999-2003. Currently, he is on the editorial boards of journals Signal Processing and Journal of Advances in Signal Processing (EURASIP), and Journal of Machine Vision and Applications (IAPR), Springer. He is a fellow of IEEE. His research interests include signal and image processing, human-computer interaction using vision and speech, audio-visual multimedia databases.